Polymer(Korea), Vol. 41, No. 3, pp. 385-393 (2017)
https://doi.org/10.7317/pk.2017.41.3.385

ISSN 0379-153X(Print)
ISSN 2234-8077(Online)

UV 경화성 수분산 폴리우레탄 아크릴레이트에 표면개질된 γ-Al_2O_3가 함유된 나노복합재료 필름의 합성과 특성

Wen Ran, Shaohui Lin, Garry L. Rempel*, and Qinmin Pan†

Green Polymer and Catalysis Technology Laboratory, College of Chemistry, Chemical Engineering and Materials Science, Soochow University

*Department of Chemical Engineering, University of Waterloo

(2016년 8월 2일 접수, 2016년 10월 8일 수정, 2016년 10월 23일 채택)

Synthesis and Properties of UV Curable Waterborne Polyurethane Acrylate Nanocomposite Films Based on the Surface Modification of γ-Al_2O_3

Wen Ran, Shaohui Lin, Garry L. Rempel*, and Qinmin Pan†

Green Polymer and Catalysis Technology Laboratory, College of Chemistry, Chemical Engineering and Materials Science, Soochow University, Suzhou 215123, Jiangsu Province, People's Republic of China

**Department of Chemical Engineering, University of Waterloo, Waterloo, Ontario N2L 3G1, Canada*

(Received August 2, 2016; Revised October 8, 2016; Accepted October 23, 2016)

Abstract: Waterborne polyurethane acrylate/surface-modified γ-Al_2O_3 (WPUA/SAl_2O_3) nanocomposite films were prepared via a UV-initiated free radical photopolymerization system composed of nanocomposite emulsion, reactive diluents and a photoinitiator. To improve the compatibility of inorganic and organic phases, γ-Al_2O_3 nanoparticles were surface-modified by γ-methacryloxypropyl trimethoxysilane and combined with a WPUA matrix. The WPUA oligomer was initially prepared by step-growth polymerization, and the content of hydrophilic chain extender, dimethylolpropionic acid (DMPA) was varied to investigate its effect on the properties of the oligomer emulsion. Performance of nanocomposite films with various loadings of SAl_2O_3 was evaluated by TGA and DSC, water uptake/swelling degree, surface wettability, tensile strength and elongation at break, etc. The results revealed that thermostability of the nanocomposite film was reinforced compared with the WPUA matrix. Swelling capacity and mechanical strength were also improved due to the increase of crosslinking density. Moreover, the optimum content of DMPA for oligomer synthesis was 5%.

Keywords: waterborne polyurethane acrylate, nanocomposite films, surface-modified γ-Al_2O_3, dimethylolpropionic acid.

Introduction

The concept of green and environmentally friendly chemistry is highly advocated in the development of the chemical industry. Waterborne polyurethanes (WPUs) cater to this idea and have been utilized in broad applications in coatings, layers, adhesive and flexible substrates.[1-4] They are extensively preferable for their outstanding properties: non-pollution, high chemical stability and easy modification.[5-8] Nevertheless, as conventional solvents are replaced by water in the synthetic process, thermostability and waterproof property of WPU are weakened to some extent, which may result in some limitations in use in many fields. Thus, the modification of WPU is required and has attracted considerable scientific attention.[9]

Many ideas have been brought up and successfully adopted to modify the WPU. For example, reactive monomers containing fluorine were introduced into the polyurethane (PU) chains to improve the waterproof property which proved applicable.[10-13] Some functional groups, such as triazine ring[14] and aromatic rings,[15] were introduced and the heat resistance property was greatly ameliorated. Acrylate monomers were commonly used to reinforce the weather resistance property.[16,17] Besides, it is believed to be an efficient way that by incorporating the surface-modified nanoparticles, an inorganic-

†To whom correspondence should be addressed.
E-mail: qpan@suda.edu.cn

organic hybrid material will be obtained.[18-21] As we know, when dispersed in the water, nanoparticles are inclined to conglomerate together due to their high surface energy, which accounts for the increase of particle size and nonuniform distribution. Hence, the surface of nanoparticles is required to be initially modified to eliminate the electrostatic interaction. Silane coupling agents are surface modifying agents, which have non-hydrolytic and hydrolytic group simultaneously. It acts like a "bridge" to combine the surface-modified nanoparticles with the WPU matrix and promote the compatibility of the inorganic and organic phases.

Nanoparticles, such as SiO_2,[22-24] ZnO,[25,26] $CaCO_3$,[27] Fe_3O_4,[28] Ag^{+}[29] and graphene[9,30] have been reported as being successfully used for the modification of PU. Similar to the other inorganic nanoparticles, Al_2O_3 has a small particle size, high mechanical strength and can be easily surface-modified. Among many crystalline forms, γ phase Al_2O_3 is an active type whose surface has an abundance of active hydroxyl groups. As for the γ-Al_2O_3 nanoparticles, γ-methacryloxypropyl trimethoxysilane (KH570) is an effective silane coupling agent for its surface modification by forming a Si-O-Al covalent bond. In this work, γ-Al_2O_3 was treated with KH570 silane coupling agent to provide better dispersion and compatibility with the WPUA matrix. The WPUA oligomer was synthesized using isophorone diisocyanate (IPDI) as a hard segment, polytetramethylene ether glycol (PTMEG) as the main soft segment and dimethylolpropionic acid (DMPA) as a hydrophilic chain extender. Based on these facts, we have prepared the nanocomposite films by merging the surface-modified γ-Al_2O_3 (SAl_2O_3) into the WPUA matrix. The effect of SAl_2O_3 quantity on the thermostability and waterproof property of the nanocomposite films was investigated. Furthermore, in order to synthesize the WPUA matrix with high performance, the effect of DMPA content on the basic properties of the WPUA oligomer emulsion was also explored to determine the optimum loading amount of DMPA.

Experimental

Materials. Isophorone diisocyanate (IPDI, AR), *N*,*N*-dimethylformamide (DMF, AR), 1,4-butanediol (BDO, AR), triethylamine (TEA, AR), oxalic acid (AR) and butyl acrylate (BA, AR) were provided by Sinopharm Chemical Reagent Co., Ltd., Shanghai. Dimethylolpropionic acid (DMPA, 99%), 2-hydroxyethyl acrylate (HEA, 99.5%), trimethylolpropane triacrylate (TMPTA, AR) and 2-hydroxy-2-methylpropiophenone (Darocur1173, AR) were obtained from Energy Chemical Reagent Co., Ltd., Shanghai. Dibutyltin dilaurate (DBTDL, 98%) and γ-methacryloxypropyl trimethoxysilane (KH570, 98%) were purchased from TCI Reagent Co., Ltd., Shanghai. Polytetramethylene ether glycol (PTMEG, Mn=2000) and γ-Al_2O_3 (10 nm, 99.99%) were supplied by Aladdin Chemical Reagent Co., Ltd, Shanghai. BA was purified using an alkaline aluminum oxide column prior to use and the other reagents were used as received without further purification.

Synthesis of KH570 Modified γ-Al_2O_3 Nanoparticles. The surface modification reaction of γ-Al_2O_3 was carried out in a three-neck flask equipped with a thermometer, a mechanical stirrer and a reflux condenser. Deionized water (10 mL), absolute ethanol (90 mL) and KH570 (0.2 g) were initially added into the flask. Oxalic acid solution (0.1 mol/L) was added as catalyst to accelerate the hydrolysis process until the pH value was about 4. After 30 min hydrolysis of KH570, γ-Al_2O_3 (1.0 g) was added at 60 °C with an agitation speed of 400 rpm for 4 h. The modified nanoparticles were washed with absolute ethanol, and separated using a centrifuge to remove the residual KH570 for three times. The white powder was finally collected and fully dried in a vacuum oven for 12 h. The mechanism of hydrolysis of KH570 is illustrated in Scheme 1.

Synthesis of the WPUA Oligomer. The WPUA oligomer was synthesized by step-growth polymerization as shown in Scheme 2, and the basic recipe for WPUA is listed in Table 1. The initial ratio (R) of [n(IPDI): n(PTMEG)] was 4, and the

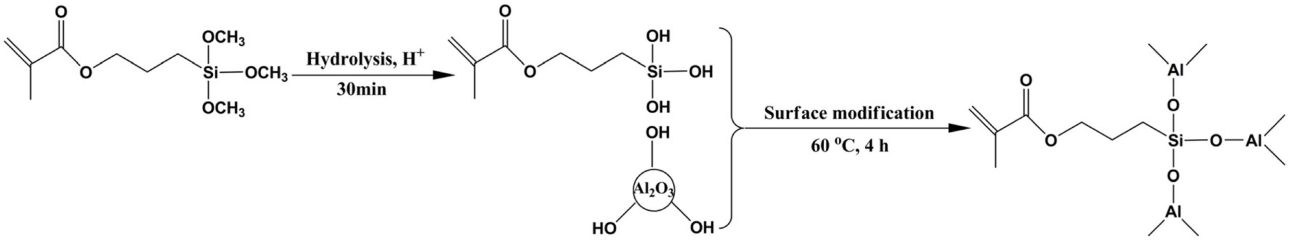

Scheme 1. Brief mechanism of hydrolysis of KH570 and surface modification of γ-Al_2O_3.

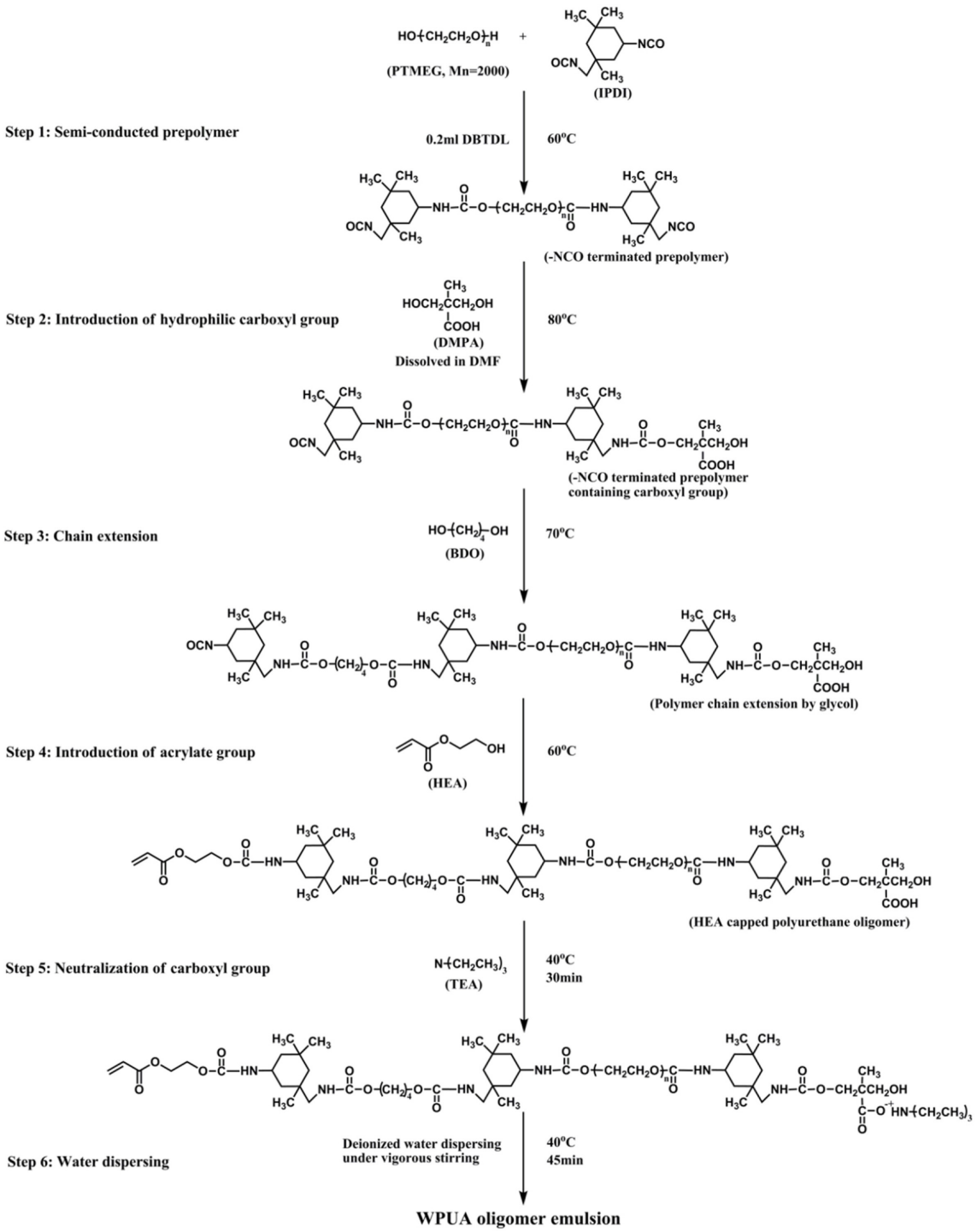

Scheme 2. Synthetic route of step-growth polymerization of WPUA oligomer.

ultimate ratio (r) of [n(-NCO): n(-OH)] was 1.2. The carboxylic acid group was thoroughly neutralized by TEA, and the reactants were dispersed into deionized water with a mass proportion of 2:3 (all monomers: water).

For further study of the step-growth polymerization process, -NCO group content was measured by di-*n*-butylamine back titration method so that the termination of each reaction step could be well controlled. The theoretical value of -NCO group

Table 1. Basic Recipe for WPUA Oligomer with Different DMPA Content

Sample	IPDI (g)	PTMEG (g)	DMPA (g)	BDO (g)	HEA (g)	TEA (g)	H_2O (g)	DMPA Content (%)
WPUA-3%	8.003	18.000	0.939	1.261	1.393	0.708	45.457	3
WPUA-4%	8.003	18.000	1.207	1.081	1.393	0.911	45.893	4
WPUA-5%	8.003	18.000	1.542	0.856	1.393	1.164	46.437	5
WPUA-6%	8.003	18.000	1.877	0.631	1.393	1.417	46.981	6
WPUA-7%	8.003	18.000	2.213	0.406	1.393	1.670	47.526	7

content (W) was calculated using the following equation:

$$W = \frac{(N_{-NCO} - \sum N_{-OH}) \times 42}{M_{-NCO} + \sum M_{-OH}} \times 100\% \quad (1)$$

where N_{NCO} is the total molar mass of the -NCO group, M_{NCO} is the mass of the monomer IPDI, $\sum N_{-OH}$ is the sum of the molar mass of hydroxyl group up to the current step, and $\sum M_{-OH}$ is the sum of the mass of monomers containing hydroxyl group up to the current step.

Preparation of WPUA/Al_2O_3 Nanocomposite Films. A calculated amount of SAl_2O_3 nanoparticles were added into the synthesized WPUA oligomer under vigorous stirring (500 rpm) at 60 °C for 2 h, and the WPUA/Al_2O_3 nanocomposite emulsion was obtained. The UV curing system was composed of the prepared emulsion, reactive diluents and photoinitiator (PI). The viscosity increased since the reactants were mixed and a gel was gradually formed. Then the gel was evenly cast onto a poly(tetrafluoroethylene) plate and dried naturally for 6 h. After the residual water was evaporated, the coating was cured by a portable UV curing machine (365 nm, 1000 W) for 30 sec to induce the photopolymerization and the nanocomposite film was prepared. The formulation of curing system is given in Table 2. BA and TMPTA were used together as co-reactive diluents, and the mass ratio of BA: TMPTA was fixed at 0.5. The mass fraction of photoinitiator was 3%.

Analysis and Characterization. Fourier transform infrared spectroscopy (FTIR) was recorded on a Nicolet is10 FTIR spectrometer (Thermo Scientific, USA) at 25 °C. Particle size and its distribution of the WPUA oligomer were measured using a Malvern Zetasizer Nano ZS dynamic light scattering (DLS, UK) at 25 °C. Thermal properties of the nanocomposite film were characterized by thermogravimetric analysis (TGA) and differential scanning calorimetry (DSC). TGA was carried out on a thermogravimetric analyzer (TG/DTA 6300, Japan) and the temperature ranged from 25 to 550 °C. DSC was executed by using TA-2000 DSC (TA instruments, USA) and the temperature range was set from 25 to 425 °C. Both of the measurements are carried out with a heating rate of 10 °C/min under a nitrogen atmosphere. Each sample taken was about 10 mg.

The WPUA oligomer emulsion was thoroughly dried in an oven at 60 °C for 12 h. Conversion of polymerization (C) and solid content of the oligomer emulsion (S) were calculated by the following equations:

$$C = \frac{M}{M_1} \times 100\% \quad (2)$$

$$S = \frac{M}{M_2} \times 100\% \quad (3)$$

where M is the mass of the oligomer emulsion after being dried, M_1 is the sum of the mass of all reactive monomers and M_2 is the mass of the oligomer emulsion before being dried.

Water uptake or swelling degree of the nanocomposite film

Table 2. Basic Formulation of WPUA/Al_2O_3 Nanocomposite Films with Different SAl_2O_3 Loadings

Sample	Oligomer (g)	BA (g)	TMPTA (g)	PI (g)	Al_2O_3 (g)	Content of Al_2O_3 (%)
WPUA/SAl_2O_3-0%[a]	12	2.67	5.33	0.36	0	0
WPUA/SAl_2O_3-0.25%	12	2.67	5.33	0.36	0.05	0.25
WPUA/SAl_2O_3-0.5%	12	2.67	5.33	0.36	0.10	0.5
WPUA/SAl_2O_3-0.75%	12	2.67	5.33	0.36	0.15	0.75
WPUA/SAl_2O_3-1%	12	2.67	5.33	0.36	0.20	1

[a]WPUA/SAl_2O_3-0%: WPUA matrix without SAl_2O_3 nanoparticles addition.

was tested as follows: the nanocomposite film was cut into 3 cm×3 cm size and soaked in the deionized water (or 5% mass fraction NaOH solution). The film was taken out after 48 h and the drips on the surface were thoroughly wiped out. The water uptake (or swelling degree), ω, was obtained by the following formula:

$$\omega = \frac{W_2 - W_1}{W_1} \times 100\% \quad (4)$$

where W_1 is the mass of the film before being put into the water (or 5% mass fraction NaOH solution) while W_2 is the mass after being taken out.

Water contact angle was measured using a JC2000C1 contact angle measurement (Powereach, China). The nanocomposite film was cut into strips and attached to glass substrates. Surface of each sample was kept smooth enough before being measured. All measurements were performed twice and the average value was used.

Tensile strength and elongation at break were recorded on a HY-930MS universal tensile testing machine (Hengyu, China). Samples were made into dumbbell shape and 30 mm long at two ends. The thickness was 0.12 mm and the width at the neck was 10 mm. Each sample was measured for three runs at 25 °C with an extension rate of 20 mm/min.

Results and Discussion

FTIR Spectra of γ-Al_2O_3 Nanoparticles. In order to confirm the modification reaction, unmodified and surface-modified γ-Al_2O_3 nanoparticles were characterized by FTIR spectra as depicted in Figure 1. Comparing these two spectra, we observed that typical absorption peaks derived from the functional group of KH570 appeared after modification. For example, 1700 and 1298 cm^{-1} were ascribed as the absorption peaks of carbonyl group and Si-O, respectively. 1635 cm^{-1} was assigned as the absorption peak of the unsaturated C=C bond. Besides, 3449 and 756 cm^{-1} were attributed to the hydroxyl group and Al-O, respectively. The result of spectral analysis demonstrated that γ-Al_2O_3 was successfully modified by the KH570 silane coupling agent.

Measurement of -NCO Group Content. As the -NCO group content always decreased after initial addition in the process of step-growth polymerization, it could be set as a criterion to determine the termination of each reaction step. The -NCO group content was measured every 30 min using a di-*n*-butylamine back titration method after polymerization began,

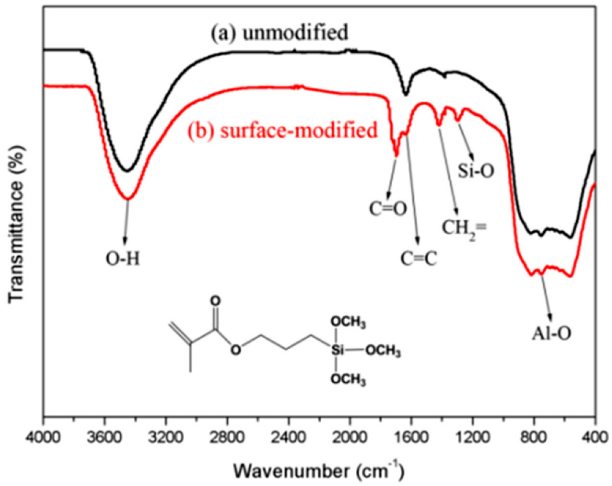

Figure 1. FTIR spectra of (a) unmodified; (b) surface-modified Al_2O_3 nanoparticles.

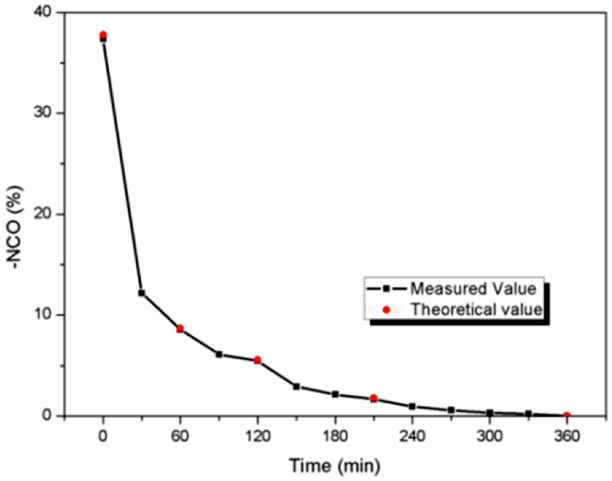

Figure 2. Theoretical and measured value of -NCO group content.

and its variation curve is displayed in Figure 2. In addition, we could also calculate the theoretical value of -NCO group content based on the recipe of WPUA oligomer as summarized in Table 3. It is assumed that a certain reaction step reached its ending on condition that the measured value of -NCO group content was lower than its theoretical value. The titration result of the -NCO group revealed that the durations for each step were 1, 1, 1.5, and 2.5 h, respectively, and the entire step-growth polymerization proceeded for about 6 h. Based on these results, it could be concluded that -NCO group content might be one of the influencing factors on the reaction rate as it decreased gradually with decreasing concentration of the -NCO group on the whole. For a certain reaction step, the reaction rate initially increased and then decreased with the addition of

Table 3. Theoretical Value of -NCO Group Content for the Termination of Each Reaction Step

Reaction step		Theoretical value[a] of -NCO group content (%)	Reaction time (h)
/	IPDI	37.79	/
Step. 1	+PTMEG	8.72	1
Step. 2	+DMPA	5.56	1
Step. 3	+BDO	1.78	1.5
Step. 4	+HEA	0	2.5

[a]Theoretical value and measured value presented in Figure 2 were obtained based on the experimental group of WPUA-5% and its recipe.

the monomer containing hydroxyl group, that is, the reaction rate changed directly with the -OH group content.

To investigate how the hydrophilic side chains of DMPA influenced the properties of the oligomer emulsion, the mass fraction of DMPA in all the reactive monomers was varied from 3 to 7% by changing the quantity of DMPA and 1,4-butanediol (BDO). Particle size and its distribution, solid content of the oligomer emulsion and the conversion of the polymerization were analyzed and discussed.

Particle Size and Its Distribution. The effect of DMPA content on particle size and distribution of the WPUA oligomer emulsion is shown in Figure 3. It can be seen from Figure 3(a) that with DMPA contents increasing from 3 to 7%, the particle sizes decreased from 77 to 24 nm. The appearance of the emulsion changed from semitransparent with blue light to almost transparent. The decrease of particle size was very fast at low DMPA content (3, 4, 5%) and slowed sown when the DMPA content was high (6 and 7%). It was implied that the introduction of the hydrophilic carboxyl group weakened the effect of twisting among PU chains and promoted the hydration of the PU macromolecules. When DMPA content reached a high level, the decrease of particle size was restricted by the increase of particle numbers and viscosity of the emulsion. The result of particle size distribution presented in Figure 3(b) was agreeable, and the relatively low particle size distribution suggested that the emulsion particles were uniform and close to being monodispersed.

Conversion and Solid Content. The conversion of the polymerization and the solid content of the oligomer emulsion were also measured with different DMPA content as depicted in Figure 4. The conversion was observed as being kept at a high level between 92.52 and 93.76%, which demonstrated that the variation of DMPA content had little influence on the polymerization conversion. For step-growth polymerization, the polymer was obtained only when the conversion was higher than 98%. Therefore, the product of this polymerization with the conversion about 93% was oligomer. The solid content of the emulsion firstly increased and then decreased with increasing DMPA content. One possible explanation for this slight change was that the solid content might be associated with the accumulating pattern of the particles. A small proportion of particles in other sizes filled in the space which was left by major particles and the overall particles were better accumulated.

When the DMPA content was 5%, the solid content reached the maximum and the conversion was also relatively high. In the meantime, particle size of the oligomer emulsion was small enough and homogeneously distributed. Taken all the factors

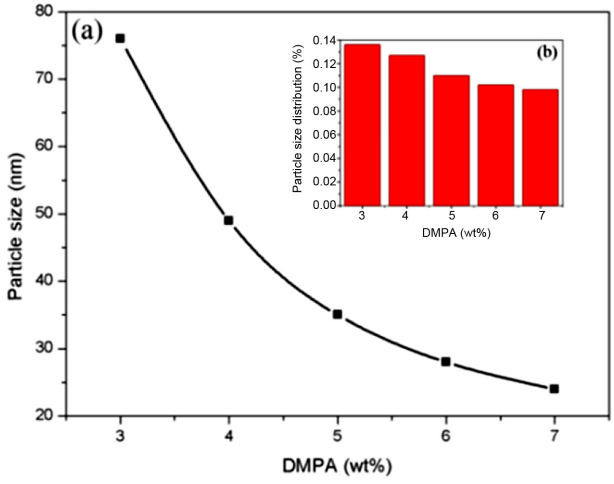

Figure 3. Particle size (a); its distribution (b) of the oligomer emulsion with different DMPA content.

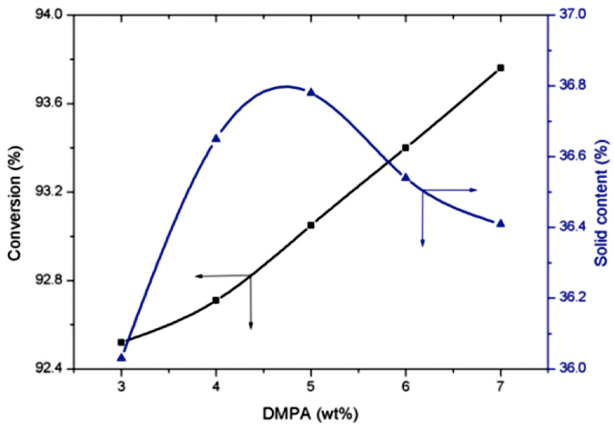

Figure 4. Polymerization conversion and solid content of the emulsion with different DMPA content.

above into consideration, it is believed that the optimum content of DMPA was 5%.

FTIR Spectrum of WPUA/SAl_2O_3 Nanocomposite Film. The structure of the WPUA/SAl_2O_3 nanocomposite film was characterized by FTIR as shown in Figure 5. The absorption peak of Al-O in both the FTIR spectra of SAl_2O_3 and the nanocomposite film demonstrated that the SAl_2O_3 nanoparticles were successfully bonded with the WPU matrix. The absorption peak of the isocyanate group at 2265 cm^{-1} and C=C at 1635 cm^{-1} disappeared after the UV curing process, which indicated the nanocomposite film was perfectly cured. 1110 and 1237 cm^{-1} were thought to be the absorption peaks of C-O and C-N, respectively. 3325 and 1529 cm^{-1} were ascribed to the N-H absorption peak. The analysis result of the FTIR spectrum implied that the WPUA/SAl_2O_3 nanocomposite film was well prepared.

Based on the previous conclusion, the WPUA oligomer used for the UV curing system was synthesized with 5% DMPA content. To study the effect of SAl_2O_3 nanoparticles on the properties of the nanocomposite film, the loadings of SAl_2O_3 were set as 0, 0.25, 0.5, 0.75 and 1% respectively. Thermal properties, waterproof property, swelling capacity, surface wettability and mechanical properties were characterized and tested.

Thermal Properties. Thermal properties of nanocomposite films were characterized by TGA and DSC analysis as shown in Figure 6 and Figure 7. It is seen in Figure 6(a) that, as expected, thermostability of the nanocomposite film was reinforced with the increased loading of SAl_2O_3. Temperature of 5% weight loss was elevated from 191 to 248 ºC, and the complete decomposition temperature was increased from 446 to 497 ºC. It was believed that the SAl_2O_3 nanoparticles were combined with the PU chains by covalent bonds during the curing process, which could provide many effective crosslinking points and act as fillers in the crosslinking structure of the nanocomposite film.[23] Accordingly, the crosslinking density was increased and thermostability was reinforced.

TGA curve of UV-WPUA/SAl_2O_3-0.75% was separated in Figure 6(a) for further study and Figure 6(b) showed the decomposition process of the nanocomposite film. The observation of two platforms in the figure suggested two stages were involved in the thermolysis process. It was demonstrated that the structure of the nanocomposite film had slight microphase separation which was mainly due to the thermodynamic incompatibility of hard and soft segments. At first, diisocyanate mostly decomposed until the occurrence of another platform and then the polyether glycol decomposed.[14] Microphase separation of soft and hard segments were favorable to

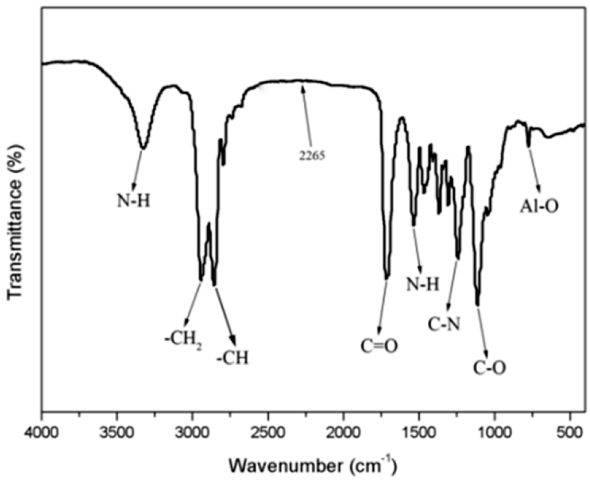

Figure 5. FTIR spectrum of the WPUA/SAl_2O_3 nanocomposite film.

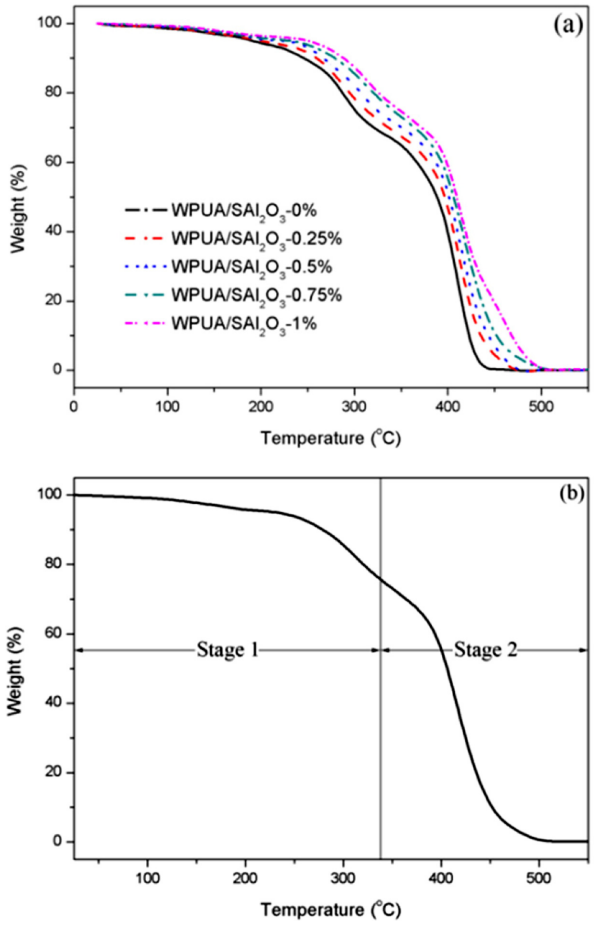

Figure 6. TGA thermograms (a); decomposition process (b) of WPUA/SAl_2O_3 nanocomposite films.

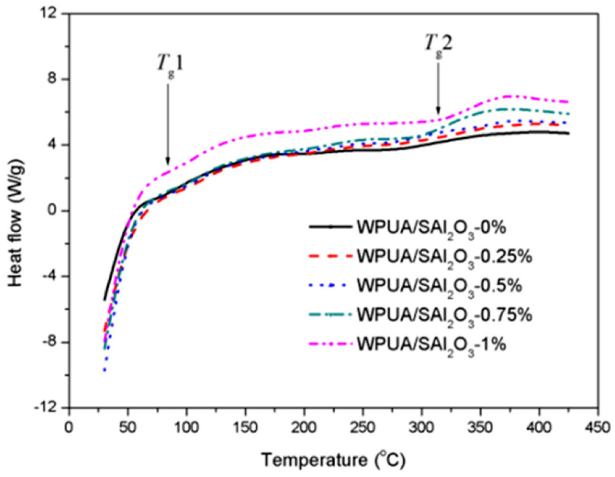

Figure 7. DSC thermograms of WPUA/SAl$_2$O$_3$ nanocomposite films.

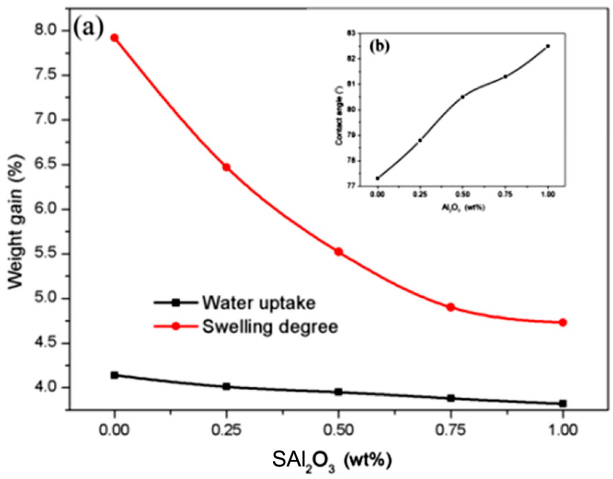

Figure 8. Water uptake/swelling degree (a); contact angle (b) of WPUA/SAl$_2$O$_3$ nanocomposite films.

Table 4. Glass Transition Temperature (T_g) of WPUA/Al$_2$O$_3$ Nanocomposite Films

Sample	T_g1 (°C)	T_g2 (°C)
WPUA/SAl$_2$O$_3$-0%	73	276
WPUA/SAl$_2$O$_3$-0.25%	75	283
WPUA/SAl$_2$O$_3$-0.5%	74	284
WPUA/SAl$_2$O$_3$-0.75%	73	304
WPUA/SAl$_2$O$_3$-1%	78	309

enhance the thermostability of the nanocomposite film.[31]

DSC analysis was applied to the measurement of the glass transition temperature (T_g). The DSC curves of the nanocomposite films with different loadings of SAl$_2$O$_3$ are presented in Figure 7. It can be seen from the figure that the DSC curves shifted towards the endothermic direction twice during the total heating process, which indicated that two T_gs were observed. One (T_g1) was observed in the low temperature zone and the other (T_g2) in the high temperature zone. T_g values of nanocomposite films are summarized in Table 4. It was clear that T_g1 was around 75 ℃ and varied little while T_g2 was improved from 276 to 309 ℃ with the increased loading of SAl$_2$O$_3$. It might be concluded from the DSC result that the bonding points of SAl$_2$O$_3$ and the WPUA matrix were mostly at the soft segment. The crosslinking density was specially strengthened at the soft segment and T_g2 was consequently improved.

Waterproof Property, Swelling Capacity and Surface Wettability. The effect of SAl$_2$O$_3$ loadings on water uptake/swelling degree and contact angle is depicted in Figure 8. Figure 8(a) showed that the water uptake degree remained at a low level ranging from 3.82 to 4.14%, which demonstrated the WPUA matrix itself possessed a desirable waterproof property and the crosslinking density was believed to be high enough to resist water. Hence, the promotion of the waterproof property was not very remarkable. On the other hand, the swelling degree of the nanocomposite films was apparently improved, decreasing from 7.92 to 4.13%. For the WPUA matrix, it exhibited slightly swollen as the covalent bonds were partly destroyed. It could come to the similar conclusion that the introduction of the SAl$_2$O$_3$ contributed much to forming a better crosslinking structure and the nanoparticles existed as fillers in the organic matrix as previous analysis showed. The surface wettability was characterized by a contact angle test as shown in Figure 8(b). The contact angle was varied over the range from of 77.3° to 82.5°, which indicated that the surface compactness was slightly promoted as well. Even though, further improvement is still required to transform the hydrophilic materials to hydrophobic ones in future work.

Mechanical Properties. Mechanical properties of the nanocomposite film were characterized by tensile strength and elongation at break. The results shown in Figure 9 indicated that the tensile strength was reinforced from 3.66 to 5.17 MPa, while the elongation at break decreased from 6.74 to 4.72% with the increased loading of SAl$_2$O$_3$. It was believed that the increase of the crosslinking density caused the polyurethane chain more rigid and uneasy to move or extend. The flexibility of the polymer chains was weakened and mechanical strength was enhanced.

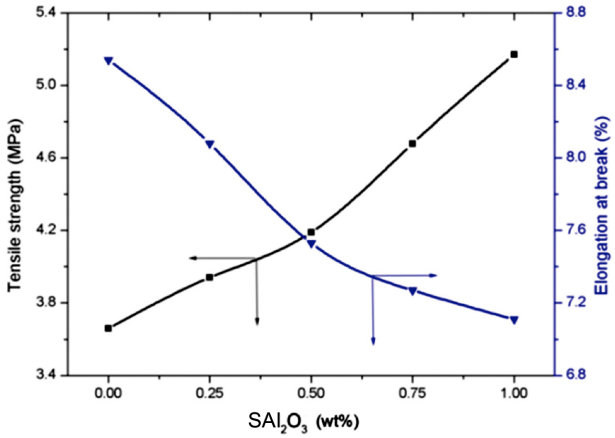

Figure 9. Tensile strength and elongation at break of WPUA/SAl_2O_3 nanocomposite films.

Conclusions

WPUA/SAl_2O_3 nanocomposite films were successfully prepared using UV curing technology by incorporating γ-Al_2O_3 nanoparticles surface-modified by KH570 into the WPUA matrix. The structure of the SAl_2O_3 and nanocomposite film was confirmed by FTIR. SAl_2O_3 nanoparticles were introduced as fillers in the WPUA matrix and the crosslinking density of nanocomposite films was enhanced because of the extra supplement of unsaturated C=C bonds by KH570. After the modification by SAl_2O_3, thermostability of the nanocomposite film was greatly improved which was verified by TGA and DSC analyses. Swelling capacity and mechanical properties were also promoted on account of the increased crosslinking density. For the synthesis of WPUA oligomer, the optimum content of DMPA was 5%. The WPUA matrix itself exhibited excellent waterproof property, but further improvement is required to promote its swelling capacity and surface wettability.

Acknowledgments: Financial support from the National Nature Science Foundation of China (No. 21176163; No. 21576174), Suzhou Industrial Park, the Priority Academic Program Development of Jiangsu Higher Education Institutions and the Program of Innovative Research Team of Soochow University are gratefully acknowledged.

References

1. H. P. Xu, F. X. Qiu, Y. Y. Wang, W. L. Wu, D. Y. Yang, and Q. Guo, *Prog. Org. Coat.*, **73**, 47 (2013).
2. A. Asif, W. F. Shi, X. F. Shen, and K. M. Nie, *Polymer*, **46**, 11066 (2005).
3. K. B. Li, Y. D. Shen, G. Q. Fei, H. H. Wang, and J. Y. Li, *Prog. Org. Coat.*, **78**, 146 (2015).
4. S. H. Yoon and B. K. Kim, *Polym. Bull.*, **68**, 529 (2012).
5. J. H. Jeon, Y. G. Park, Y. H. Lee, D. J. Lee, and H. D. Kim, *J. Appl. Polym. Sci.*, **132**, 42168 (2012).
6. H. D. Hwang, C. H. Park, J. I. Moon, H. J. Kim, and T. Masubuchi, *Prog. Org. Coat.*, **72**, 663 (2011).
7. J. M. Park, Y. H. Lee, H. Park, and H. D. Kim, *J. Appl. Polym. Sci.*, **131**, 40603 (2014).
8. J. C. Liu, Q. H. Liu, X. F. Zheng, R. Liu, Q. D. Mu, and X. Y. Liu, *Polym. Bull.*, **73**, 647 (2016).
9. J. H. Xu, X. Cai, and F. L. Shen, *Appl. Surf. Sci.*, **379**, 433 (2016).
10. Y. K. Cho and W. K. Lee, *Polym. Korea*, **40**, 439 (2016).
11. S. R. Kim, J. Y. Park, S. G. Lee, and J. D. Lee, *Polym. Korea*, **39**, 902 (2015).
12. T. C. Canak and I. E. Serhatli, *Prog. Org. Coat.*, **76**, 388 (2013).
13. J. M. Park, J. H. Jeon, Y. H. Lee, D. J. Lee, H. Park, H. H. Chun, and H. D. Kim, *Polym. Bull.*, **72**, 1921 (2015).
14. Z. H. Fang, H. Y. Duan, Z. H. Zhang, J. Wang, Y. X. Huang, D. Q. Li, Y. X. Huang, J. J. Shang, and Z. Y. Liu, *Appl. Surf. Sci.*, **257**, 4765 (2011).
15. Z. H. Fang, J. J. Shang, Y. X. Huang, J. Wang, D. Q. Li, and Z. Y. Liu, *Express. Polym. Lett.*, **4**, 704 (2010).
16. C. Decker, F. Masson, and R. Schwalm, *Polym. Degrad. Stabil.*, **83**, 309 (2004).
17. X. Wang, Y. Hu, L. Song, W. Y. Xing, H. D. Lu, P. Lv, and G. X. Jie, *J. Polym. Res.*, **18**, 721 (2011).
18. H. G. Kim and K. E. Min, *Polym. Korea*, **39**, 256 (2015).
19. H. G. Kim, *Polym. Korea*, **40**, 9 (2016).
20. W. C. Lin, H. Yang, T. L. Wang, Y. T. Shieh, and W. J. Chen, *Express. Polym. Lett.*, **6**, 2 (2012).
21. J. W. Xu, W. M. Pang, and W. F. Shi, *Thin Solid Films*, **514**, 69 (2014).
22. D. W. Nam, B. U. Nam, B. J. Cha, and B. J. Kim, *Polym. Korea*, **31**, 111 (2007).
23. B. Seo, S. Park, S. Kim, and K. R. Ha, *Polym. Korea*, **40**, 421 (2016).
24. S. W. Zhang, A. X. Yu, X. Q. Song, and X. Y. Liu, *Prog. Org. Coat.*, **76**, 1032 (2013).
25. D. Kim, K. Jeon, Y. Lee, J. Seo, K. Seo, H. Han, and S. Khan, *Prog. Org. Coat.*, **74**, 435 (2012).
26. R. S. Mishra, A. K. Mishra, and K. V. S. N. Raju, *Eur. Polym. J.*, **45**, 960 (2009).
27. K. H. Nam, K.Seo, J. Seo, S. H. Khan, and H. Han, *Prog. Org. Coat.*, **85**, 22 (2015).
28. S. L. Chen, S. D. Zhang, Y. F. Li, and G. H. Zhao, *Rsc Adv.*, **5**, 4355 (2015).
29. R. D. Toker, N. K. Apohan, and M. V. Kahraman, *Prog. Org. Coat.*, **76**, 1243 (2013).
30. X. Wang, W. Y. Xing, L. Song, B. Yu, Y. Hu, and G. H. Yeoh, *React. Funct. Polym.*, **73**, 854 (2013).
31. S. H. Ra, H. D. Lee, and Y. H. Kim, *Polym. Korea*, **39**, 579 (2015).